Supplementary Materials

2 Supplementary Tables

4 Supplementary Figures

Supplementary Table 1

Table S1: Table of mice entered into in vivo histological experiments

Genotype	Age at infection (in weeks)	Length of infection (in weeks)	N
Shi/shi x Rag2$^{-/-}$	16	3-4	3
Shi/shi x Rag2$^{-/-}$	13	6	5
Shi/shi x Rag2$^{-/-}$	11-12	8	5
Shi/shi x Rag2$^{-/-}$	8-9	11-12	5
Total shiverer transplants			**18**
Rag1$^{-/-}$ only	16	12	5
Total myelin wild-type transplants			**5**

Table S2. Mutations of the VP1 gene in infected human glial chimeric mice

Length of infection (wks)	Age at infection (wks)	Host genotype	Non-synonymous mutations occurring more than once (number of occurrences)	Total number of non-synonymous mutant VP1 sequences
3.5	16.1	shi/rag2-/-	-	17
8	11.6	shi/rag2-/-	G8del (2) S72Y (9) S61L (5) R266T/G (6)	42
11.6	8.1	shi/rag2-/-	V233I (3) S123C (3)	18
11.6	8.1	shi/rag2-/-	G57S (2) D66G (2) Y38A (2) V156A (2) L354P (2) E328G (2)	18
12	16.4	rag1-	K60Q (2) F68L (7) S123C (7) G125V (3)	30
Starting virus			H122Y/P(3)	4

The VP1 gene is mutated in the glial chimeric mouse brain following infection with JCV

Human GPC-engrafted shiverer/rag2-null or normally myelinated rag1-null mice were infected with the Mad-1 variant of JCV for periods of time ranging from 4-12 weeks. TA PCR cloning was used to sequence JCV VP1 DNA from 96 viral clones/mouse, taken at three different anteroposterior levels (anterior forebrain, the site of JCV injection, and posterior forebrain). Among the 384 clones sequenced from the 4 JCV-injected mice, 129 VP-1 mutations were noted relative to the initial sequence of wild-type type 1A (Mad-1) JCV. Of the 129 muteins, 15 were represented two or more times in the overall set. Mutations that occurred more than once in a single animal are listed, with the number of mutations in parentheses. Note that S123C and D66G have been reported in PML(26).

Supplementary Figures

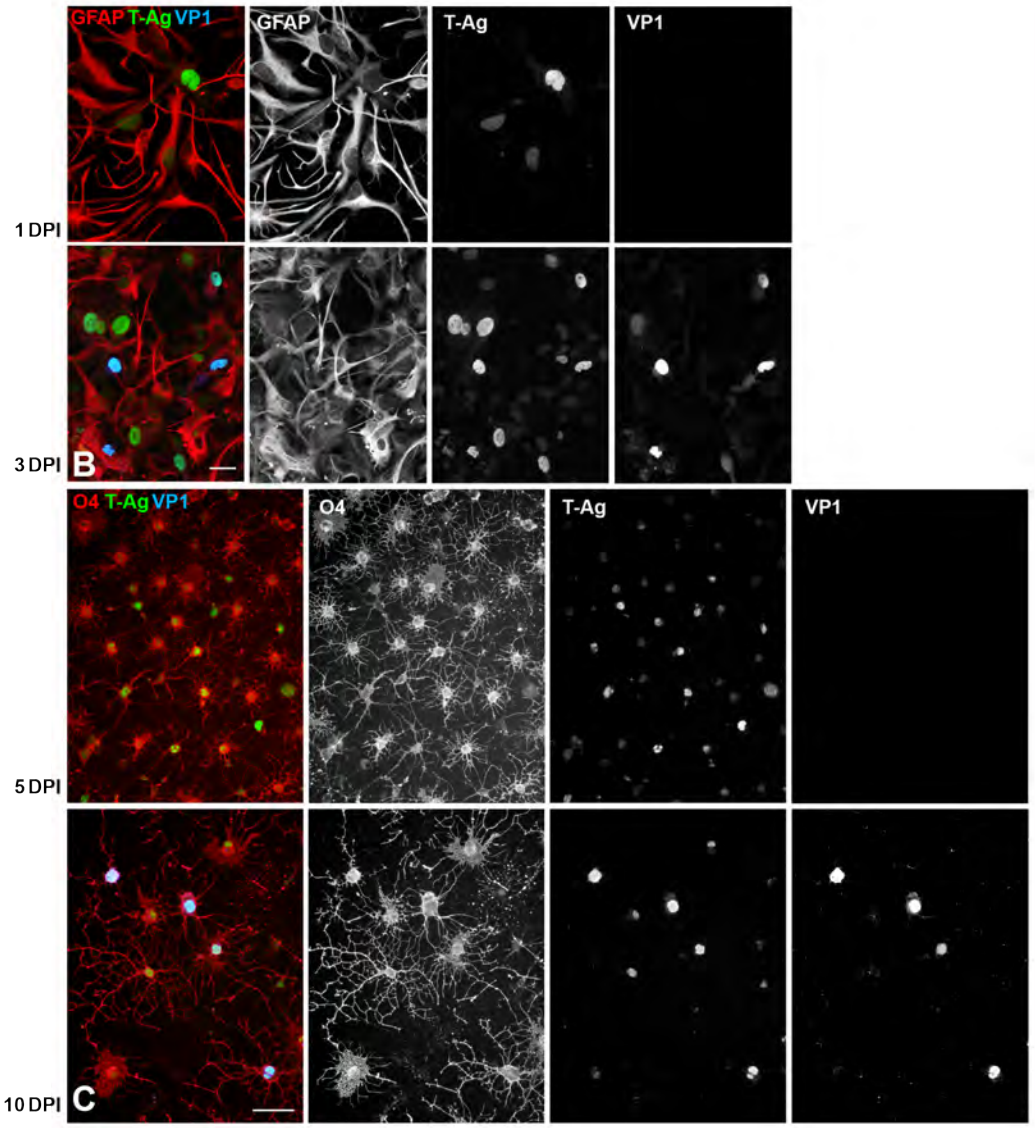

Figure S1. Oligodendrocytic JCV infection was delayed relative to that of astrocytes in vitro

These images, Supplementary to and following the plate designations of **Figures 1B** and **1C**, show that T antigen was expressed as early as 1 DPI in CD44-sorted GFAP$^+$ astrocytes, whereas VP1 was first expressed at 3 DPI (**B,** shown as individual immunolabels comprising the composite of **Figure 1B**). In contrast, oligodendrocytic infection in vitro, as shown in **C**, which includes the individual color splits of **Figure 1C**, was both delayed and of relatively low efficiency, showing weak T antigen expression without VP1 at 5 DPI (*arrowheads*), with VP1$^+$ oligodendroglia appearing only at 10 DPI. In contrast to the rapid course of astroglial infection, oligodendrocytic infection was thus delayed and initially of relatively low efficiency.

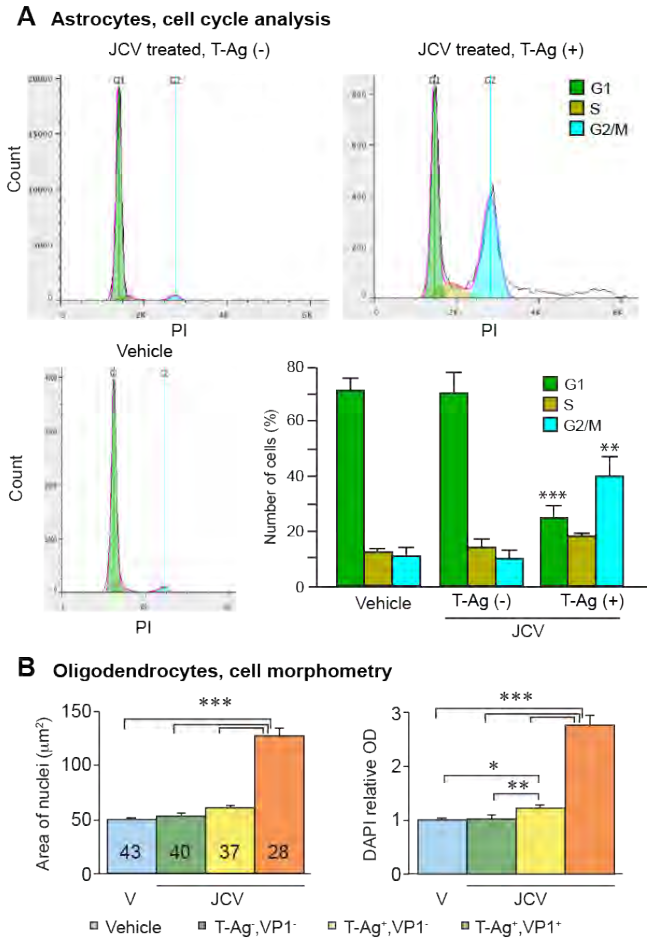

Figure S2. JCV infected glia exhibited G2 cell cycle arrest

A, Infected astrocytes exhibit G2 accumulation. Cell cycle analysis of JCV-infected human astroglia, derived from GPCs exposed to high serum for 10 days, then exposed to JCV and analyzed 14 days later. The relative percentages of cells in each stage of cell cycle were compared between vehicle-treated and JCV-infected astrocytes, using the Dean-Jett-Fox model in FlowJo. This analysis revealed that JCV-infected, T antigen$^+$ astrocytes exhibited a marked accumulation of cells in G2 relative to uninfected controls.

B, Infected oligodendrocytes, like astroglia, manifest nuclear hypertrophy. Morphometry revealed that VP1-expressing oligodendrocytic nuclei were typically enlarged relative to those of uninfected cells (*graph, right*), and had significantly higher DNA content (*graph, left*). Photo-micrographs of O4$^+$ oligodendrocytes were recorded with a constant exposure time for the DAPI signal. Areas and total fluorescence intensities of DAPI$^+$ nuclei were analyzed using ImageJ (v.1.45s).

Data are represented as means ± SEM from 3 experiments. Numbers in bars indicate the numbers of analyzed nuclei. One-way ANOVA followed by Bonferroni post-hoc test. p* < 0.05, p** < 0.01, p*** < 0.001.

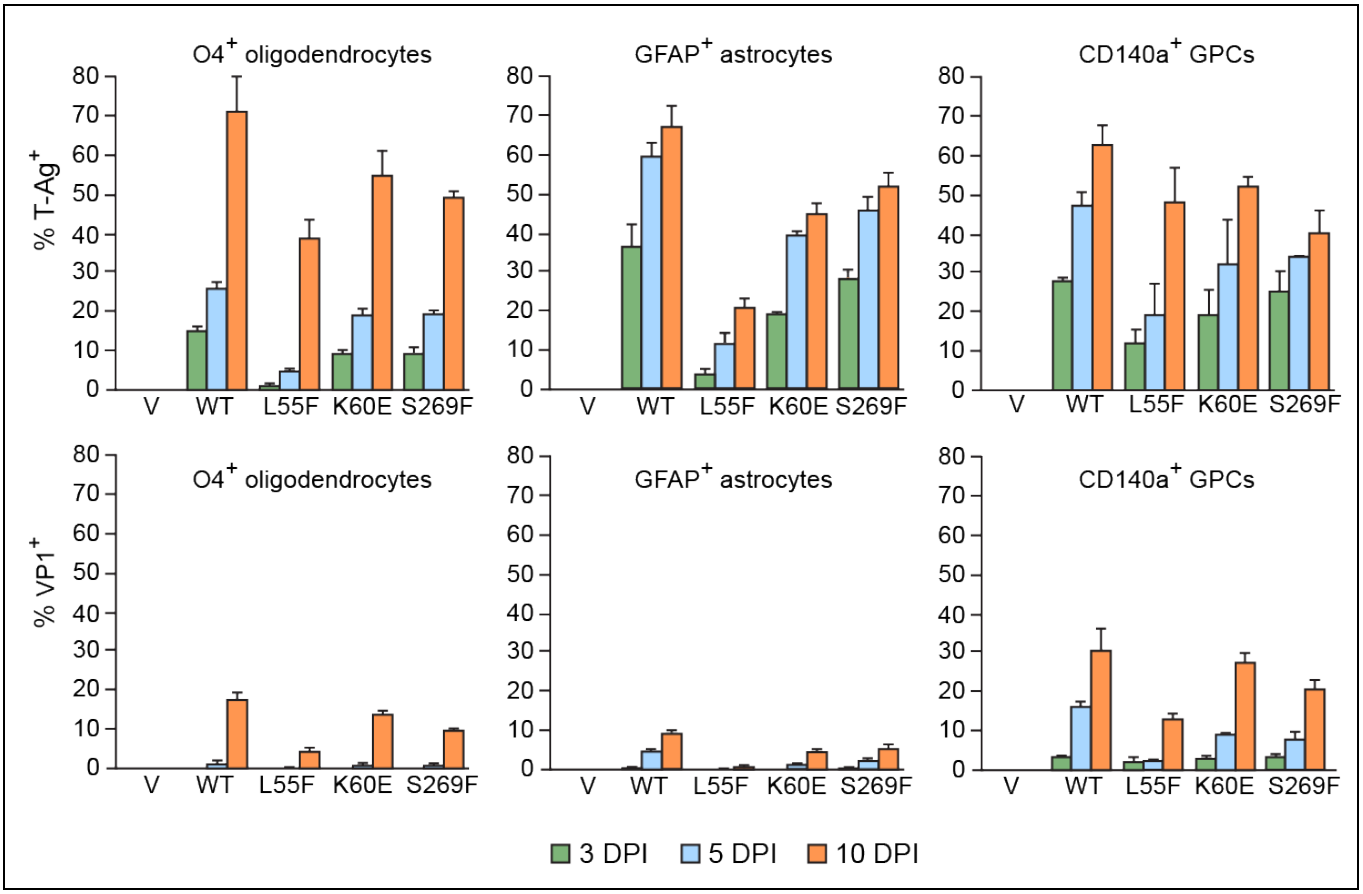

Figure S3. In vivo infection by JCV mutants

Infectivity of type 2A (Mad-1 NCCR) JCV VP1 mutants in oligodendrocytes, astrocytes, and GPCs in vitro. The VP1 mutants infected each tested cell type less efficiently than did wild-type JCV; the L55F mutein was the least effective. Nonetheless, by 10 DPI, all cell types were robustly infected by each tested VP1 mutein. JCV propagated more effectively in OPCs than in astrocytes. For example, 3.5% of type 2A WT JCV-infected OPCs expressed VP1 as early as 3 DPI, whereas only 0.2% of astrocytes were $VP1^+$ at that early time-point.

Data are mean ± SEM (n = 4/group, triplicate wells).

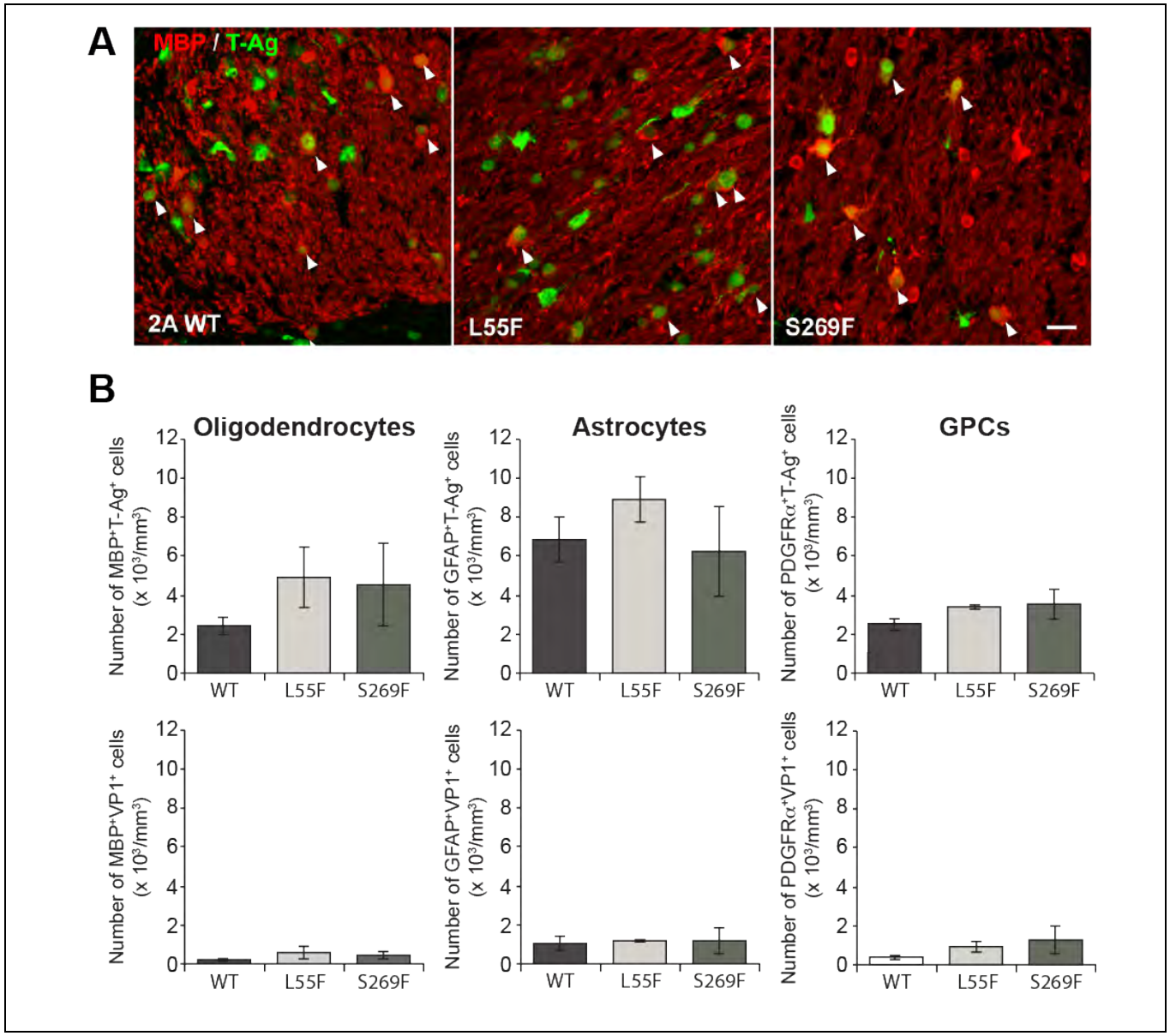

Figure S4. In vivo infection by JCV mutants

JCV VP1 mutants manifested no phenotypic preferences in vivo. Type 2A (Mad-1 NCCR) JCV with WT or mutant VP1 was injected into the corpus callosum of human glial chimeric shiverer x rag2-null mice at 17 weeks of age, and the mice killed 5 weeks later. **A**, MBP^+ mature oligodendrocytes in the corpus callosum were infected by WT virus and both the L55F and S269F muteins equally. **B**, Quantification of $T\text{-}Ag^+$ and $VP1^+$ infected cells in the corpus callosum. Using one-way ANOVA, no statistically significant differences were noted in the infectivity of these viral genotypes ($p > 0.05$ for all comparisons). Means ± SEM, corrected for the number of human nuclear $antigen^+$ cells (n = 3-5).